J Mar Sci Technol (2013) 18:339–348
DOI 10.1007/s00773-013-0211-8

ORIGINAL ARTICLE

Estimation and prediction of effective inflow velocity to propeller in waves

Michio Ueno · Yoshiaki Tsukada · Katsuji Tanizawa

Received: 15 May 2012 / Accepted: 14 January 2013 / Published online: 7 February 2013

Abstract A free running test using a container ship model clarified properties of effective inflow velocity to propellers in waves. The analysis assumes that thrust and torque vary keeping their relation to the effective inflow velocity as represented by open-water characteristics of a propeller in a steady calm water condition. Measurement in regular waves confirmed the variation of average values of the effective wake coefficient and ship speed depending on wavelength and wave encounter angle. Comparison with the longitudinal flow velocity measured at the sides of the propeller using an onboard vane-wheel current meters confirmed that one can estimate the effective inflow velocity based on thrust or torque data. Theoretical estimates in regular waves based on a strip method are provided and compared with the experimental data. A prediction model of the future inflow velocity is proposed to cope with a time delay of a propeller pitch controller for higher propeller efficiency in waves.

Keywords Effective inflow velocity in waves · Free running model test in waves · Thrust and torque in waves · Effect of propeller load on wake coefficient · AR model · Burg method

1 Introduction

Higher propulsive efficiency of ships has become more important than ever as one of the measures to prevent global warming. There are many measures to reduce the fuel consumption such as development of hull forms having small resistance, high efficiency propellers, and devices to reuse heat or fluid energy otherwise discarded.

Among them is a propeller pitch control based on a real time estimate of effective inflow velocity to the propeller that depends on ship speed, ship motion, and waves. In case there is a time delay caused by the estimation procedure or the mechanism in the pitch controller, one must predict future inflow velocity to the propeller.

Taniguchi [1] and McCarthy et al. [2] reported open-water characteristics of a propeller in waves, where they fixed the propeller to the carriage. Nakamura et al. [3] studied open-water characteristics of a propeller in regular and irregular waves considering the effect of heave, pitch and surge oscillations. They showed that the average propeller characteristics in waves are identical with those in calm water. They also clarified the fluctuation of thrust and torque in waves trace on open-water curves. Yamanouchi et al. [4] and Yoshino et al. [5] reported experimental results on the thrust and torque fluctuation in waves using free running models. Sluijs [6] and Nakamura et al. [7] used in their experiments captive models in which vertical motions were free. Nakamura et al. [8], Tsukada et al. [9], and Aalbers and Gent [10] reported the wake flow measurement in waves at the propeller position using towed model ships without a propeller. The former two papers confirmed the average wake coefficient in regular waves varies depending on wavelength. Nakamura et al. [8] pointed out the average wake coefficient in irregular waves is the same in general as that in the calm water. Tasaki [11] discussed theoretically effects of surge motion and orbital motion of waves on the effective inflow velocity. Nakamura et al. [7] considered the effects of heave and pitch motion. These are researches forming a basis for this

M. Ueno (✉) · Y. Tsukada · K. Tanizawa
Fluids Engineering and Ship Performance Evaluation Department, National Maritime Research Institute, 6-38-1 Shinkawa, Mitaka, Tokyo 181-0004, Japan
e-mail: ueno@nmri.go.jp
URL: http://www.nmri.go.jp/

paper but no research intended to estimate the inflow velocity in real time using thrust or torque data and use it to improve the propeller efficiency.

The authors carried out a free running model test from the viewpoint of estimating axial inflow velocity of a propeller in waves. The thrust and torque data and open-water characteristics of a propeller in steady calm water provide direct estimates of the inflow velocity. This process assumes that a quasi-steady analysis works even in unsteady conditions. A strip method provides theoretical estimates of inflow velocity and ship motion in regular waves. The authors discuss whether the direct and the theoretical estimation are practical in actual seas. Data of relative longitudinal flow velocity at the sides of the propeller in regular and irregular waves measured using vane-wheel current meters corroborate the discussion. The authors propose a method to predict the inflow velocity in the near future using past data to cope with a possible time delay of a pitch controller.

2 Model test

2.1 Model ship and test conditions

The test site is the Actual Sea Model Basin [12], completed in 2010, where 382 units of flap type wave generators surround the whole periphery of the tank except the adjacent trim tank part. The carriage system consists of a main and a sub carriage with a turntable that can tow or track a model ship.

The authors carried out a free running test using a container ship model. Table 1 lists the principal dimensions of the model ship compared with the actual one, in which L stands for the length between perpendiculars. The model ship runs along designated courses by a self-steering control while the carriage system tracks it using a CCD camera. Although cables connect the model ship to the carriage, they are loose enough not to restrain the ship's motion. Four wires clamp the model ship for acceleration and deceleration, which are also loose enough during measurement.

Table 2 shows the test conditions. A servomotor drove the propeller at two kinds of constant revolutions n, 11.9 and 16.6 rps. The wave encounter angle χ varies from 0 deg. following the wave condition, to a 180 deg. head wave condition, at intervals of 45 deg. In regular wave conditions, designated wave heights H_w were 0.05 m and 0.075 m and the wavelength to ship length ratio λ/L varied from 0.4 to 3.0. The spectra of long crested irregular waves are the types of the International Ship Structure Congress [13] of which wave period T_{01} are 1.0, 1.3 and 1.6 s, where their designated significant wave heights were the same, 0.1 m.

The authors also carried out conventional towing tests; resistance tests, self-propulsion tests, and propeller tests in open water, to analyze the free running test data, though they do not appear explicitly in this paper.

2.2 Measuring instruments

Table 3 shows measured items and measuring instruments in the tank test. The model ship setup is shown in Fig. 1.

Table 1 Principal dimensions of a container ship

Item	Ship	Model
Length between P. (m), L	300.0	4.000
Breadth (m)	40.0	0.533
Draft (m)	14.0	0.187
Block coefficient	0.65	
Prop. diameter (m)	9.0	0.120
Expanded area ratio	0.775	

Table 2 Free running test conditions

Item	Parameter	
Propeller revolution, n (rps)	11.9	16.6
Ship speed in calm water (m/s)	0.991	1.394
Froude number, F_n, in calm water	0.158	0.223
Wave encounter angle, χ (deg.)	0 (following)–180 (head)	
Regular wave		
Wave height, H_w (m)	0.05, 0.075	
Wave length ship length ratio, λ/L	0.4–3.0	
Irregular wave		
Wave spectrum (long crested waves)	ISSC	
Wave period, T_{01} (s)	1.0, 1.3, 1.6	
Significant wave height, $H_{1/3}$ (m)	0.10	

Table 3 Measured items and devices in the free-running model test

Item	Device
Ship position and speed	Tracking system
Ship motion	Fiber optical gyro
Thrust and torque	Dynamometer
Longitudinal flow velocity (314 mm right and 320 mm left off the propeller center)	Vane-wheel current meter (3 mm diameter)
Encounter wave	Wave gauge (servo type, fixed to the sub-carriage)
Relative wave height (fore-end centerline and AP both sides)	Wave gauge (capacity type, fixed to the model)
Rudder angle	Potentiometer

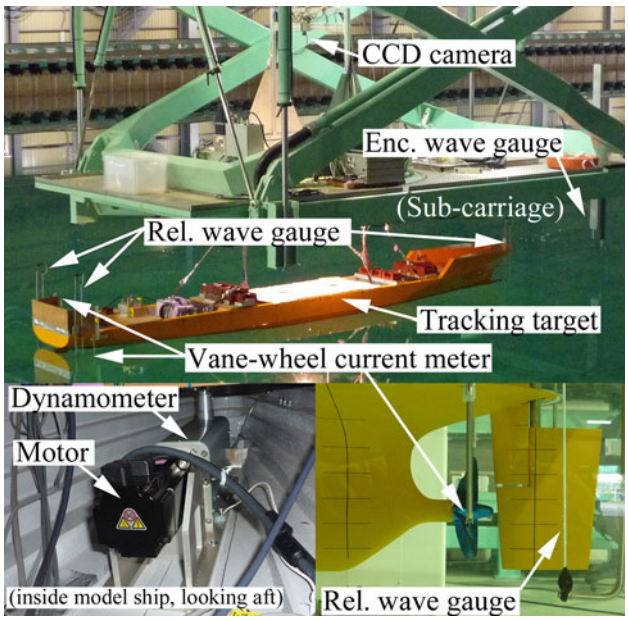

Fig. 1 Model ship setup under the sub-carriage

According to towing test data [12], maximum position errors of the carriage are about 0.003 m, 0.002 m, and 0.02 deg. for the main and sub carriages and turntable, respectively. Maximum speed errors are about 0.004 m/s, 0.004 m/s, and 0.1 deg./s. The CCD camera fixed to the turntable watches tracking targets onboard, two black circles of which the diameter is 0.08 m on a white board, located along the centerline, 0.4 m fore and aft from the center of gravity of the model ship. The image analysis tells position and heading of the model ship relative to the carriages, on which data the model ship tracking is based. Resolutions of an image are 640 × 480 pixels. Since the distance of the circles is about 80 % of 640 pixels, maximum position and direction errors are about 0.002 m and 0.11 deg., respectively. Frequency of analysis that depends on the size of the circles is about 20 Hz. The authors used 20 Hz data of position and speed stored in files; on the other hand, they monitored these data in real time with other data measured at 20 Hz.

The fiber optical gyro measures pitch, roll, and yaw angles and rates together with surge, sway, and heave accelerations.

The vane-wheel current meters fixed to the model ship are for comparison with the estimated effective inflow velocity converted from the thrust and torque data. Frequency responses of the current meters were tested separately by towing them in regular waves. The results tell the variation of amplitude ratio and phase delay is not significant within the frequency range of free running test.

2.3 Thrust and torque data corrections

The mass of the propeller and shaft, 0.803 kg in the model test, affects the thrust data in pitch and surge oscillating motion. The effect was estimated using longitudinal acceleration data and subtracted from measured thrust data. Since the accelerometer was fixed to the model ship, measured longitudinal acceleration involves surge and pitch effects combined. Maximum thrust corrections in $H_w = 0.05$ m conditions were 1.8 and 1.0 % of the steady thrust in calm water with $n = 11.9$ and $n = 16.6$ rps, respectively.

Suppose the added mass is half the water sphere, of which the diameter is equal to that of the propeller, multiplied by the expanded area ratio, it should be 0.351 kg. This implies the added mass effect of the propeller disk should be smaller than half the shaft and propeller mass effect, if corrected. Based on the rough estimate above, the authors did not take the effect into consideration.

The authors also corrected torque data by subtracting propeller shaft friction calibrated depending on propeller revolution using a dummy boss. The friction component varies from 1.2 to 2.3 % of the measured torque.

3 Estimation using thrust and torque data

3.1 Procedure for estimating effective inflow velocity

In ordinary self-propulsion tests in calm water, thrust or torque data tell the effective inflow velocity using the open-water characteristics of the propeller. These are the thrust or torque identification methods. Although the phenomenon in waves, considered here, is unsteady, the authors applied the same procedure to every instantaneous measured datum in waves and discuss validity of this procedure.

In this paper, 'wake coefficient' and 'effective wake coefficient' mean $1 - w_p$ in which w_p stands for an effective wake fraction.

3.2 Average wake coefficient in regular waves

Data in regular waves are unsteady but periodic. In this subsection, properties of the average effective wake coefficient in waves are discussed.

Ship speed decreases in waves because of the resistance increase in waves. Speed decrease is significant in head wave conditions, as shown in Fig. 2, especially where the wavelength to ship length ratio is around one. Applying the thrust and torque identification methods and averaging after that provides average wake coefficients in waves shown in Fig. 3. The effective inflow velocity analyzed

using torque data is larger than those using thrust data. In general, the effective wake coefficient obtained by the thrust identification method is more reliable in model tests. However, the torque identification method should be more practical since torque data is more reliable than thrust for full-scale ships.

The average wake coefficient in waves becomes larger than in calm water admittedly in head wave conditions where the speed decrease is large. Figure 4 shows the average wake coefficient's dependency on Froude number in head waves of various wavelength and wave heights 0.05 and 0.075 m, which suggests that the larger the propeller load is the larger then is the average wake coefficient. The authors think this is the same mechanism as wake coefficient's variation in calm water measured in a propeller load varying test by Hinatsu et al. [14] and Adachi [15]. The difference is that the change of propeller load in this free running test is caused by added resistance in waves. Hinatsu et al. [14], experimentally, and Toda [16], theoretically and experimentally, explain this phenomenon in calm water is a result of deformation of boundary layer due to the propeller load. The wave and ship motion effect on the average nominal wake coefficient is discussed in references [8, 9].

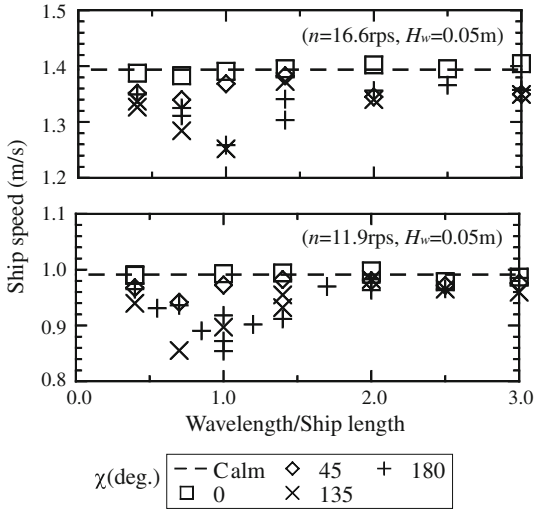

Fig. 2 Average model ship speed in regular waves (n, propeller revolution; H_w, designated wave height; χ, wave encounter angle)

3.3 Time varying inflow velocity in irregular waves

Figure 5 shows the time varying inflow velocity o fthe propeller converted from thrust and torque data. Relative flow velocity measured by the current meters and ship speed are also shown for comparison. The incident waves are long-crested irregular waves of which the wave encounter angle χ is 180 deg., head wave condition, wave period T_{01} is 1.3 s and significant wave height is 0.1 m. The propeller revolution is 11.9 rps. These data are typical examples in its non-periodicity and unsteadiness.

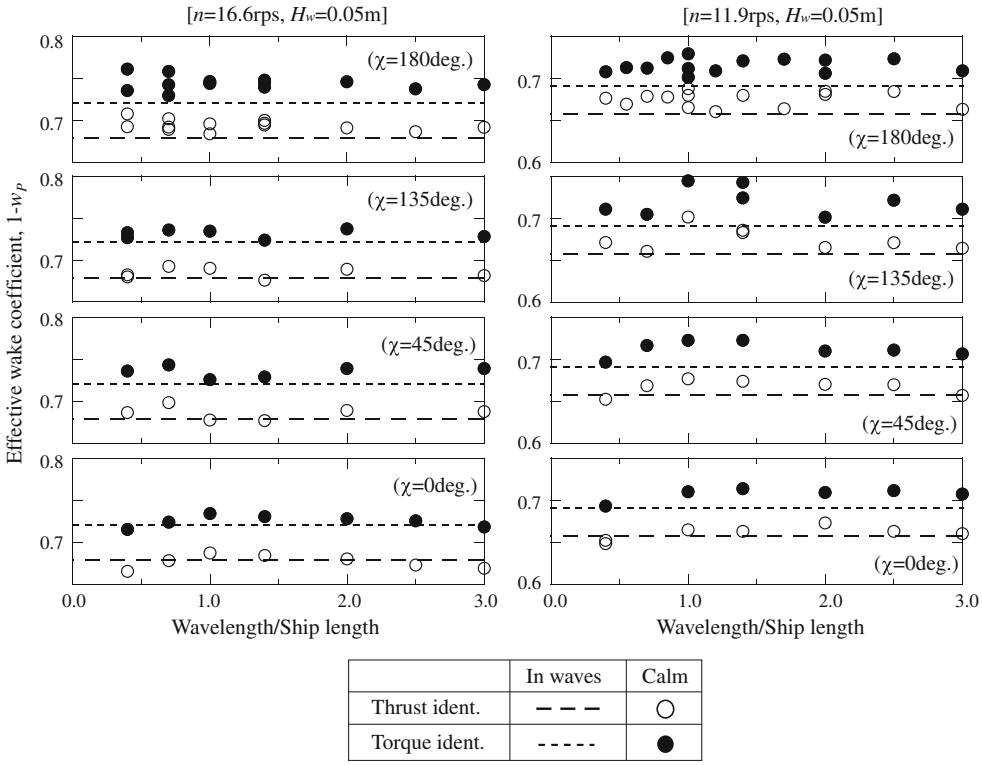

Fig. 3 Average wake coefficient, $1 - w_P$, in regular waves obtained by thrust and torque identification method, dependency on wavelength to ship length ratio (n, propeller revolution; H_w, designated wave height; χ, wave encounter angle)

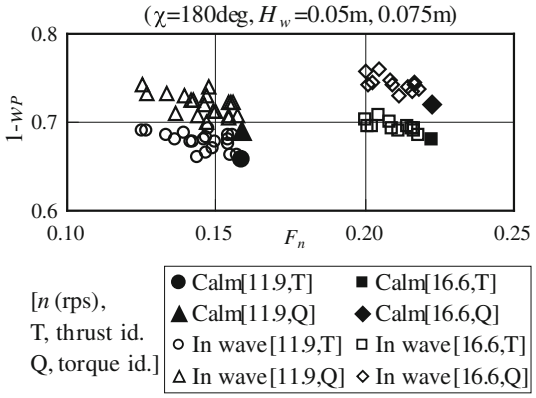

Fig. 4 Average wake coefficient, $1 - w_P$, in regular waves obtained by thrust and torque identification method, dependency on Froude number, F_n (χ, wave encounter angle; H_w, designated wave height; n, propeller revolution)

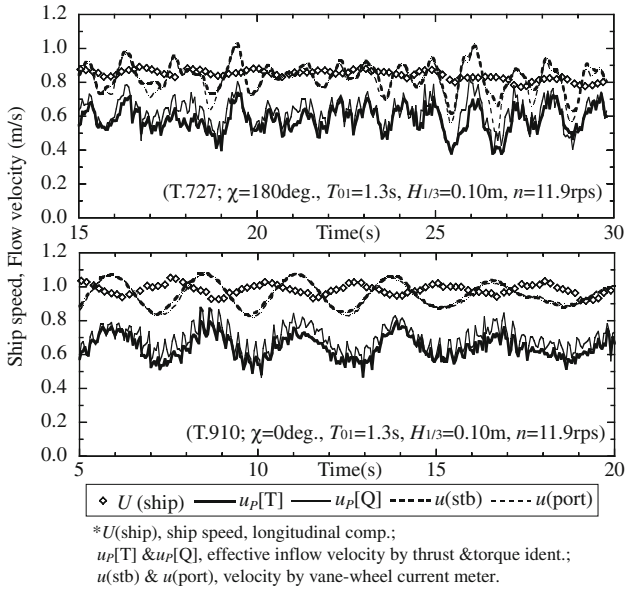

*U(ship), ship speed, longitudinal comp.;
u_P[T] &u_P[Q], effective inflow velocity by thrust &torque ident.;
u(stb) & u(port), velocity by vane-wheel current meter.

Fig. 5 Time history of longitudinal component of ship speed, U (ship); effective inflow velocity obtained using thrust and torque data, u_P[T] and u_P[Q]; flow velocity measured by vane-wheel current meter at starboard and port sides of propeller, u(stb) and u(port) in irregular head and following waves (χ, wave encounter angle; T_{01}, primary wave period; $H_{1/3}$, designated significant wave height; n, propeller revolution)

The model ship speed varies due to surge motion in waves. The relative flow velocities fluctuate around the model ship speed, which is a result of a water particle's orbital motion due to waves. The reason why the averages of these fluctuations are seen to be slightly smaller than the model ship speed is that the current meters are in the wake flow near the model ship's side hull. The inflow velocities converted from thrust and torque data shows almost the same values. These time varying characteristics resemble those of the relative flow velocities though there are quantitative differences . These quantitative differences should come from those of wakes at the center of and the 314 or 320 mm off center of the propeller position.

Figure 6 shows comparison of an auto correlation coefficient and a cross correlation coefficient for confirming the resemblance. The auto correlation is of the thrust converted inflow velocity. The cross correlation coefficient is of the thrust converted inflow velocity and the starboard relative flow velocity. Some phase shift that could be partly attributed to phase delay of the current meter is seen between these two coefficients, but the two correlation coefficients agree well. The authors consider that this result supports the fact that the thrust or torque converted inflow velocity is reliable even in unsteady conditions.

Based on the discussion above, the direct estimate of inflow velocity using thrust or torque is promising for application to a propeller pitch control at actual seas though it cannot tell future values.

4 Estimation using wave data

Average ship speed, ship motion in waves, and orbital motion of water particles due to waves determine the effective inflow velocity to the propeller. Since theoretical calculations can estimate the ship motion in waves, it can also estimate the inflow velocity in waves based on incident wave information. This section looks into whether this procedure works or not.

Let us consider the inflow velocity in regular waves of which amplitude is h_a, wave number k, and wave circular frequency ω. Figure 7 shows a coordinate system in which positive directions for surge, heave, and pitch motions are forward, downward, and bow up, respectively. Their phase, measured from when wave trough is at midship, takes a positive value for delay.

Wave encounter circular frequency ω_e, defined by the following equation, depends on wave encounter angle χ and average ship speed U.

$$\omega_e = \omega - kU\cos\chi. \tag{1}$$

Suppose that surge, heave and pitch amplitudes are ξ_a, ζ_a and θ_a; their phase delays ε_ξ, ε_ζ and ε_θ; the propeller coordinates (x_P, 0, z_P). Then the following formula is considered to estimate the inflow velocity u_P, in which t represents time.

$$\begin{aligned} u_P = {} & (1 - w_P)\{U - \omega_e\xi_a \sin(\omega_e t - \varepsilon_\xi)\} \\ & + \omega h_a \exp[-k\{z_P + \zeta_a \cos(\omega_e t - \varepsilon_\zeta) \\ & - x_P\theta_a \cos(\omega_e t - \varepsilon_\theta)\}]\cos\chi \\ & \times \cos[\omega_e t - k\cos\chi\{x_P - \xi_a \cos(\omega_e t - \varepsilon_\xi)\}]. \end{aligned} \tag{2}$$

In Eq. 2, the effective wake coefficient $(1 - w_P)$ is assumed to include its propeller load dependency. Surge

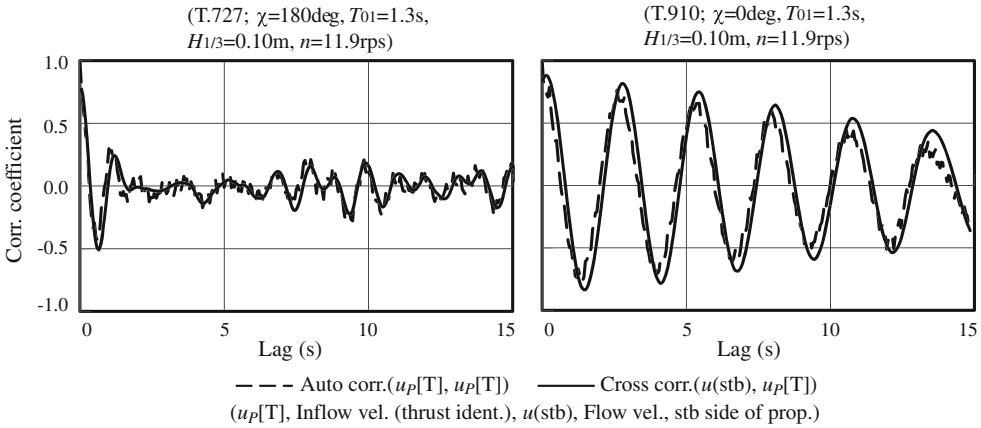

Fig. 6 Comparison of auto correlation coefficient of effective inflow velocity obtained using thrust data, u_P[T], and cross correlation coefficient of u_P[T] and flow velocity measured by vane-wheel current meter at starboard side of propeller, u(stb) in irregular head and following waves (χ, wave encounter angle; T_{01}, primary wave period; $H_{1/3}$, designated significant wave height; n, propeller revolution)

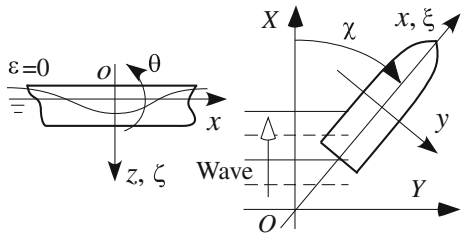

Fig. 7 Coordinate system (OXY, Earth fixed coordinate system; oxyz, ship fixed coordinate system; χ, wave encounter angle; ξ, surge; ζ, heave; θ, pitch; ε, phase of ship response)

motion affects ship velocity and the longitudinal position of the propeller. Heave and pitch motions affect the vertical position of the propeller.

The authors confirmed through trial calculations that the effects of oscillation of the propeller position or the effect of pitch and heave motion are negligible. Neglecting the effect and introducing a coefficient α representing the effect of wave amplitude decrease at the stern, pointed out by Jinnaka [17, 18], lead to the following equation.

$$u_P = (1 - w_P)\{U - \omega_e \xi_a \sin(\omega_e t - \varepsilon_\xi)\} + \alpha\omega\, h_a \exp(-kz_P)\cos\chi\cos(\omega_e t - kx_P\cos\chi). \quad (3)$$

Equation 3 consists of the wake flow including the surge oscillation effect and the orbital motion of water particles in an attenuated wave at the stern. Nakamura et al. [7] adopted the effect of wave amplitude decrease at the stern by introducing a coefficient in their equations for head wave conditions. Taking into account the effect of encounter angle χ in Nakamura's coefficient, the authors assume α as follows.

$$\alpha = \begin{cases} 0.2\left(\dfrac{\lambda}{L|\cos\chi|}\right) + 0.5, & \text{for } \dfrac{\lambda}{L|\cos\chi|} \le 2.5 \\ 1, & \text{for } 2.5 < \dfrac{\lambda}{L|\cos\chi|}. \end{cases} \quad (4)$$

Figure 8 shows the calculated surge amplitude using the strip method [19], compared with the experimental data of 0.05 m wave height. Although the average model ship speed depends on the wavelength and the encounter angle, the calculations assume the ship speed is constant for each encounter angle. The average Froude numbers, measured and used in the calculations, for the encounter angle 180, 135, 45, and 0 deg. are 0.149, 0.149, 0.155, and 0.158 for 11.9 rps and 0.212, 0.211, 0.217, and 0.233 for 16.6 rps, respectively. The calculations agree well with the experimental data, which confirms the validity of theoretical calculation.

Figure 9 presents the amplitude of the effective inflow velocity in regular waves, calculated using Eqs. 3 and 4, and obtained experimentally using thrust and torque data. In theoretical calculation, the effective wake coefficient is assumed to be 0.7. The calculation seems to explain qualitatively the test data in the long wave region. Differences between the calculation and test results, however, are not small for all wave encounter angles. Since the estimates of surge motion are fairly good as shown in Fig. 8, the estimate of wave amplitude attenuation, α in Eq. 4, should be responsible mainly for these discrepancies.

Even if a method could resolve this problem, one traditional problem remains; the estimate of wave field. It is difficult to measure in actual seas directional spectra including phase of every elementary wave. Therefore, theoretical estimate of inflow velocity is hard to apply to a propeller pitch control even though it could tell future values.

5 Prediction of effective inflow velocity

The direct estimate using thrust or torque data is practical and reasonable in actual seas on applying to a propeller pitch control. However, the direct estimate cannot tell the future inflow velocity to cope with a time delay of a pitch controller. This is the reason why the direct estimate needs a prediction model.

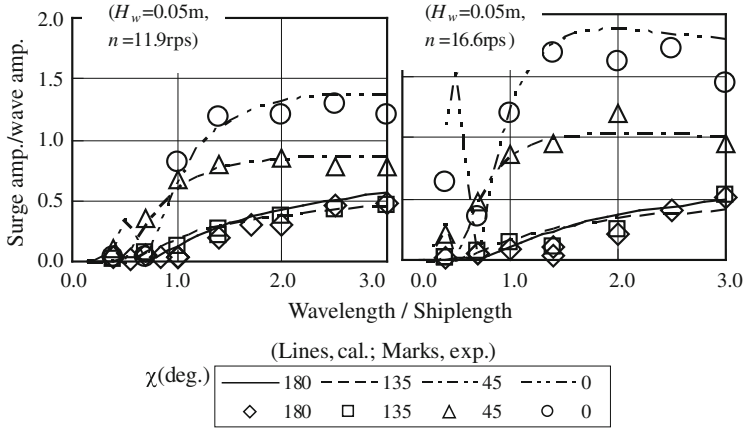

Fig. 8 Surge amplitude ratio to wave amplitude in regular waves, comparison of experimental data with calculations (H_w, designated wave height; n, propeller revolution; χ, wave encounter angle)

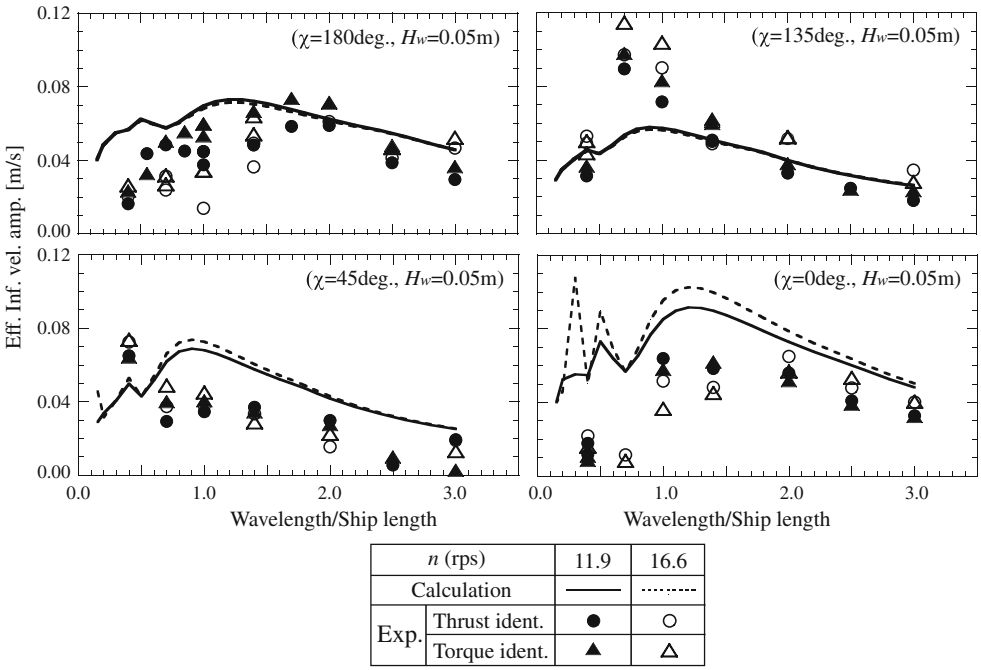

Fig. 9 Amplitude of effective inflow velocity obtained by thrust identification method (*filled marks*) and torque identification method (*open marks*), comparing with calculation (lines) (H_w, designated wave height; n, propeller revolution; χ, wave encounter angle)

Time delay of a propeller pitch control in full-scale would be several seconds. To predict several seconds' future values, the authors applied the AR (Autoregression) model using the Burg method [19] to the thrust or torque converted inflow velocity data for the prediction.

The AR model is represented by the following equation.

$$u_{P,i} = a_1 u_{P,i-1} + a_2 u_{P,i-2} + \cdots + a_{Nt} u_{P,i-Nt}. \quad (5)$$

In Eq. 5, $u_{P,i}$, (a_1, a_2,…, a_{Nt}), and N_t stand for the inflow velocity of data number i, AR coefficients, and the number of AR terms, respectively.

The procedure is as follows. At a point of time, the analysis determines AR coefficients using the most recent data of which number is N_a. The minimum Final Prediction Error determines the number of AR terms, N_t, that is, though, limited up to twice the square root of N_a [20]. The AR calculation applying the most recent past N_t data predicts a one-step future value. The AR calculation applying to the predicted one step future value and the most recent past $N_t - 1$ data predicts a two-step future value. This AR calculation procedure repeats until it reaches designated N_p-step future value. At the next point of time, on obtaining one new datum, the whole procedure above repeats.

Figure 10 shows test number 727 (T.727) in irregular head waves, the same measurement as Fig. 5; $\chi = 180$ deg., $U = 0.841$ m/s, $T_{01} = 1.3$ s, $H_{1/3} = 0.10$ m, $n = 11.9$ rps. Total data number, ND, is 597 of which the frequency is 20 Hz. Rudder angle varies slowly between -2 and 4 deg. during this measurement. Therefore, the rudder blockage effect should be negligibly small. The prediction procedure used filtered data, shown in the top figure, to see prediction errors clearly.

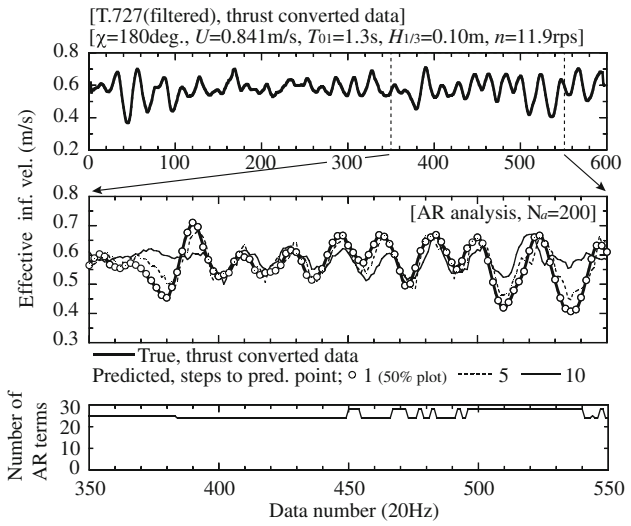

Fig. 10 Prediction of effective inflow velocity by AR model using the Burg method, compared with true thrust converted data in head irregular waves (T. no. 727; 200-point AR analysis; χ, wave encounter angle; U, ship speed; T_{01}, primary wave period; $H_{1/3}$, designated significant wave height; n, propeller revolution)

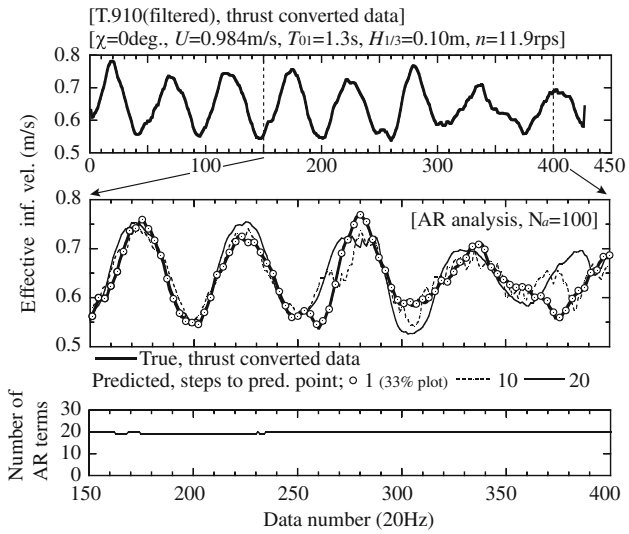

Fig. 11 Prediction of effective inflow velocity by AR model using the Burg method, compared with true thrust converted data in following irregular waves (T. no. 910; 100-point AR analysis; χ, wave encounter angle; U, ship speed; T_{01}, primary wave period; $H_{1/3}$, designated significant wave height; n, propeller revolution)

The authors had confirmed beforehand that this filtering did not affect the outcome qualitatively. The second figure shows the comparison of predicted values with true thrust converted inflow velocity data, from data number 350–550. N_a is 200 and N_p values are 1, 5, and 10. The predicted values of $N_p = 1$ are almost identical with the true data. However, the larger N_p is, the larger the discrepancy between predicted values and true data becomes, which is significant especially when the data tendency changes from the past. The bottom figure is of N_t for every AR analysis point. Most of all, the AR term number is between 24 and 28, the limit.

Figure 11 is another example of a following irregular wave condition, test number 910 (T.910); $\chi = 0$ deg., $U = 0.984$ m/s, $T_{01} = 1.3$ s, $H_{1/3} = 0.10$ m, $n = 11.9$ rps, ND = 427. N_a is 100 and N_p values are 1, 10, and 20. Rudder angle varies between 0 and 4 deg. The discrepancy between predicted values and true data is smaller relatively for N_p values than the head wave condition, Fig. 10. The reason is the true data are more periodic or monotonous and the AR model works well for this following wave condition. Most of all, the AR term number is 19 or 20, the limit.

Figure 12 shows how the root mean square of prediction error grows when the steps to the prediction point increase depending on the AR analysis number. Data ranges of error analysis are 221–578 for T.727 and 221–408 for T.910, independent of either the analysis point number or the number of steps to prediction point. The difference between head and following wave conditions are clear. Both prediction errors seem to saturate for large but at different number of steps to the prediction point.

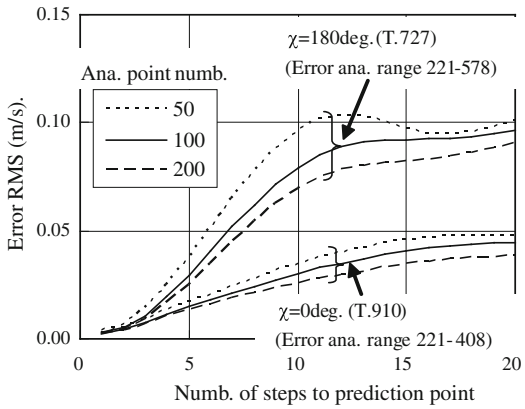

Fig. 12 Root mean square of prediction error depending on AR analysis data length and prediction point (comparison of T. no. 727 with T. no. 910; χ, wave encounter angle)

If we look into a point of the same prediction error, 0.04, for example, of which the data number of AR analysis is 100, the steps to prediction point are 6 and 15 for head and the following wave conditions, respectively. Corresponding times to the prediction point are 0.30 and 0.75 s for head and the following wave conditions. Modal wave encounter periods, on the other hand, are 0.92 and 2.52 s, respectively. The ratios of these values then become comparable to 0.33 and 0.30 for head andthe following wave conditions. Based on an assumption that an allowable time is one third the wave encounter period, it would be, in full-scale, 2.7 s in head waves and 7.3 s in following waves, respectively, for the above examples. For a cargo

carrier with a 4-blade controllable pitch propeller, of which length, dead weight, propeller diameter, and maximum continuous output are 120 m, 11400 ton, 3.6 m, and 3.9 MW, respectively, the time delay of pitch controller is around 1.7 s and the pitch control speed is 1 deg./s. These values seem to suggest this prediction model works well as long as the time delay is concerned.

The encounter wave period, however, could be smaller than these examples above depending on wave period, ship speed, and encounter angle. In case the allowable time becomes smaller than the time delay of a pitch controller, the prediction model may not work well. Therefore, analyzing the wave encounter period will help in actual seas in advising whether the model should be on or off.

The prediction model presented here is simple because it employs only estimated inflow velocity. The Kalman filter combined with the AR model [21] or with the principal component analysis [22] might improve the prediction because they can use information such as ship speed or relative wave height, which the authors leave to future study.

6 Concluding remarks

To realize a propeller pitch control that can respond to varying inflow velocity to propeller in waves, its estimation and prediction are studied.

A free running model test was carried out to estimate the unsteady inflow velocity to a propeller in waves. The authors used an ordinary thrust and torque identification method to analyze the unsteady inflow velocity though these direct methods which are originally for steady calm water conditions. The average effective wake coefficient shows the propeller load dependencies, which are analogous to those observed in propeller load varying tests in calm water. Relative longitudinal flow at the sides of propeller show close correlation with the estimated inflow velocity, confirming the direct method works well even in unsteady conditions. Theoretical estimates in regular waves based on a strip method are also provided and compared with the direct estimates. Differences between them implied the need of improvement in evaluating wave amplitude's attenuation at stern.

To cope with a time delay of a propeller pitch controller, the authors proposed a prediction model of the inflow velocity using an AR model. Applications of the method to the model ship data in irregular waves confirmed that it could cope with a possible time delay of the controller in actual seas depending on a wave encounter period.

Acknowledgments The authors thank Mr. Yasushi Kitagawa at the National Maritime Research Institute for his providing the information about a propeller pitch controller of a cargo carrier. This study was supported by the Program for Promoting Fundamental Transport Technology Research from the Japan Railway Construction, Transport and Technology Agency (JRTT).

Appendix

Reference test data including ship motion in regular and irregular waves are shown in Figs. 13 and 14.

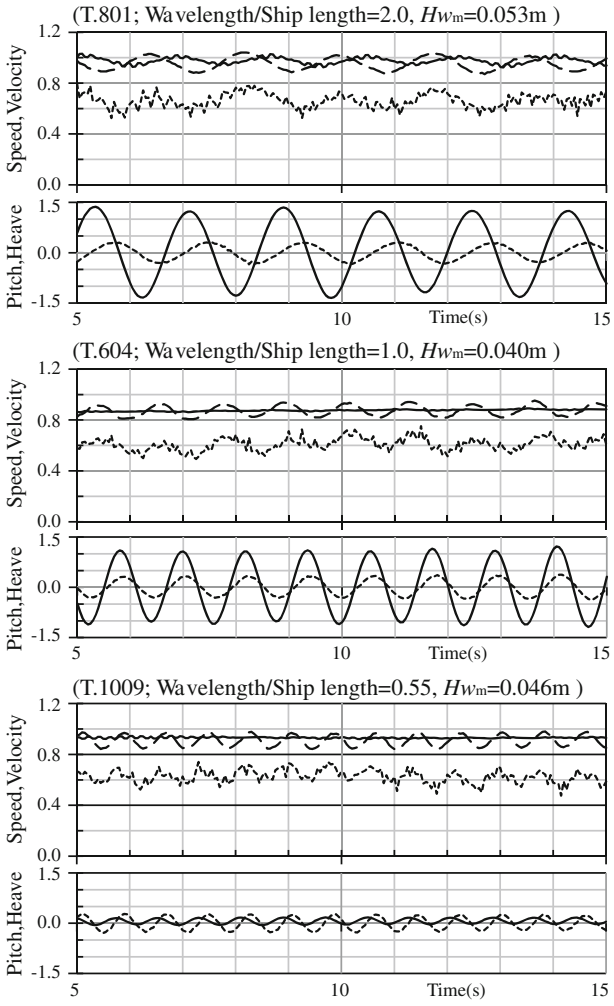

Fig. 13 Time history of longitudinal component of ship speed, U(ship); effective inflow velocity obtained using thrust data, u_P[T]; flow velocity measured by vane-wheel current meter at starboard, u(stb) in regular head waves (χ, wave encounter angle; Hw_m, measured wave height; n, propeller revolution)

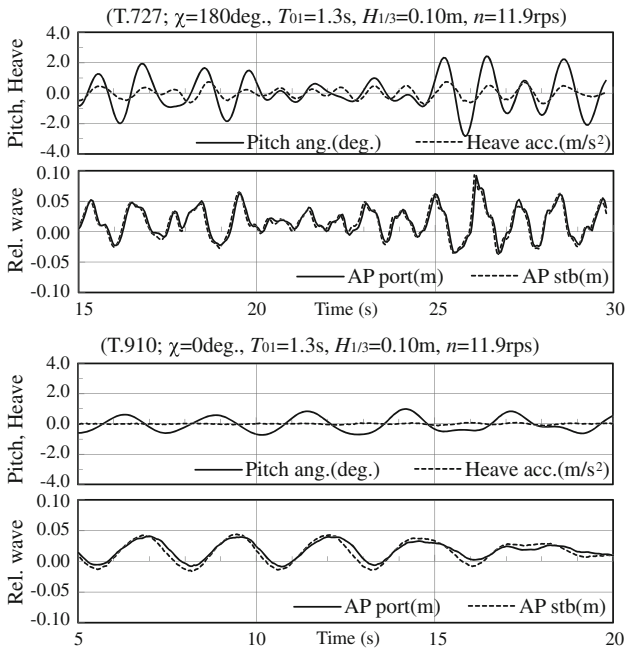

Fig. 14 Time history of pitch angle (*bow-up positive*), heave acceleration at center of gravity (*downward positive*), and relative waves at aft perpendicular (*upward positive*) in irregular waves, corresponding Fig. 5; (χ, wave encounter angle; T_{01}, primary wave period; $H_{1/3}$, designated significant wave height; n, propeller revolution)

References

1. Taniguchi K (1961) Propulsion performance in waves. Bull Soc Naval Archit Japan 383:315–328 (in Japanese)
2. McCarthy JH, Norley WH, Ober GL (1961) The performance of a fully submerged propeller in regular waves. David Taylor Model Basin, Report 1440
3. Nakamura S, Naito S, Inoue R (1975) Open-water characteristics and load fluctuations of propeller in waves. J Kansai Soc Naval Archit Japan 159:41–55 (in Japanese)
4. Yamanouchi Y, Ando S (1966) Experiments on a Series 60, CB = 0.70 ship model in oblique regular waves. Papers of Ship Research Institute, No. 18
5. Yoshino T, Saruta T, Yoshino Y (1974) Model tests on thrust and torque increase and fluctuations acting on the propeller shafts of high-speed container ships with single or twin screws in oblique waves. Papers Ship Res Inst 11(4):217–232 (in Japanese)
6. Sluijs MFV (1972) Performance and propeller load fluctuations of a ship in waves. Netherlands Ship Research Centre TNO, Report No. 163S
7. Nakamura S, Hosoda R, Naito S (1975) Propulsive performance of a container ship in waves (3rd Report). J Kansai Soc Naval Archit Japan 158:37–46 (in Japanese)
8. Nakamura S, Hosoda R, Naito S, Inoue M (1975) Propulsive performance of a container ship in waves (4th Report). J Kansai Soc Naval Archit Japan 159:29–39 (in Japanese)
9. Tsukada Y, Hinatsu M, Hasegawa J (1997) Measurement of unsteady ship wakes in waves. J Kansai Soc Naval Archi Japan 228:15–20 (in Japanese)
10. Aalbers AB, Gent WV (1985) Unsteady wake velocities due to waves and Motions measured on a ship model in head waves. In: Proceedings of 15th symposium on naval hydrodynamics, vol 15, pp 69–81
11. Tasaki R (1957) On the characteristics of the driving machine in the self-propulsion test among waves. J Soc Naval Archit Japan 101:25–32 (in Japanese)
12. Tanizawa K, Ueno M, Taguchi H, Fujiwara T, Miyazaki H, Sawada H, Tsukada Y (2010) The actual model ship basin. Papers Natl Marit Res Inst 10(4):1–40 (in Japanese)
13. International Ship Structure Congress (1964) Report of the committee 1, Environmental conditions. In: Proceedings of the 2nd ISSC
14. Hinatsu M, Moriyama F, Tsukada Y, Adachi H (1982) On a correlation between a propeller load and stern flow variation. In: Proceedings of the General Meeting of Ship Research Institute vol 40, pp 86–89 (in Japanese)
15. Adachi H (1983) On the theoretical bases and application methods of the propeller load varying test method. J Soc Naval Archit Japan 154:109–117 (in Japanese)
16. Toda Y, Tanaka I, Iwasaki Y (1982) Distortion of axisymmetric boundary layer due to propeller suction. J Kansai Soc Naval Archit Japan 185:39–48 (in Japanese)
17. Jinnaka T (1958) Some experiments on the exiting forces of waves acting on the fixed ship models. J Soc Naval Archit Japan 103:47–57 (in Japanese)
18. Jinnaka T (1960) Periodic sources and its applications (continued). J Soc Naval Archit Japan 108:1–4 (in Japanese)
19. Salvesen N, Tuck EO, Faltinsen M (1970) Ship motions and sea loads. Trans Soc Naval Archit Marine Eng 78:250–287
20. Hino M (1977) Spectrum analysis. Asakura Shoten (in Japanese)
21. Tanizawa K, Minami Y (2006) Wave impact avoidance system for ships. Japan Patent JP2008-44472A
22. Hashimoto N, Nagai N, Shimizu K, Sugawara K (1996) On the Reliability of the statistical wave forecasting through Kalman filtering combined with principal component analysis. Report of the Port and Harbour Research Institute, 35-1, pp 91–115 (in Japanese)